SUPPLEMENTARY DATA

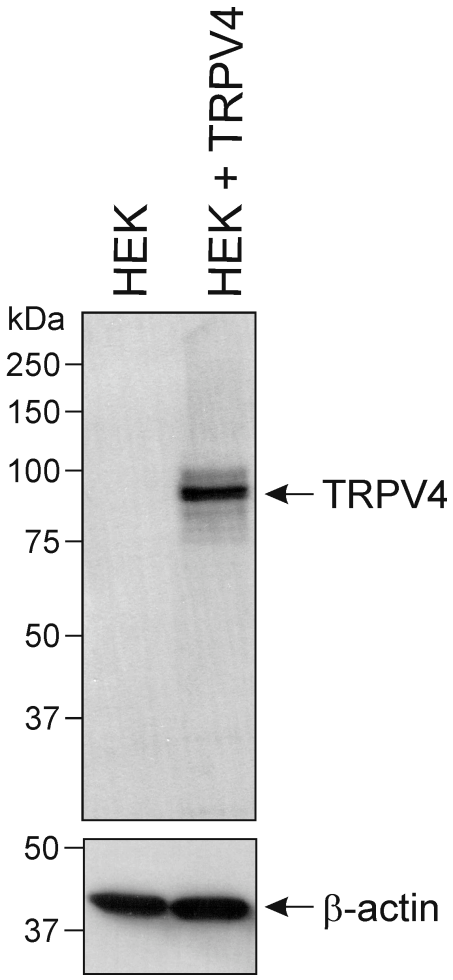

Supplementary Figure 1: Whole cell extracts from HEK-293 cells transfected or not with the mice TRPV4-expressing vector were separated by SDS-polyacrylamide gel electrophoresis, blotted on the PVDF membrane and used for immunodetection with affinity purified anti-TRPV4 antibodies. A band of about 90-95 kDa, which correspond to predicted molecular weight of TRPV4, was only detected in TRPV4-transfected HEK-293 cells. Weak immunostained bands in the close proximity of main TRPV4 signal most likely correspond to the post-translationally modified TRPV4 proteins since they were

not present in not-transfected HEK-293 cells. To visualize equal loading of proteins, the blotting membrane was re-probed with monoclonal anti β-actin antibodies.

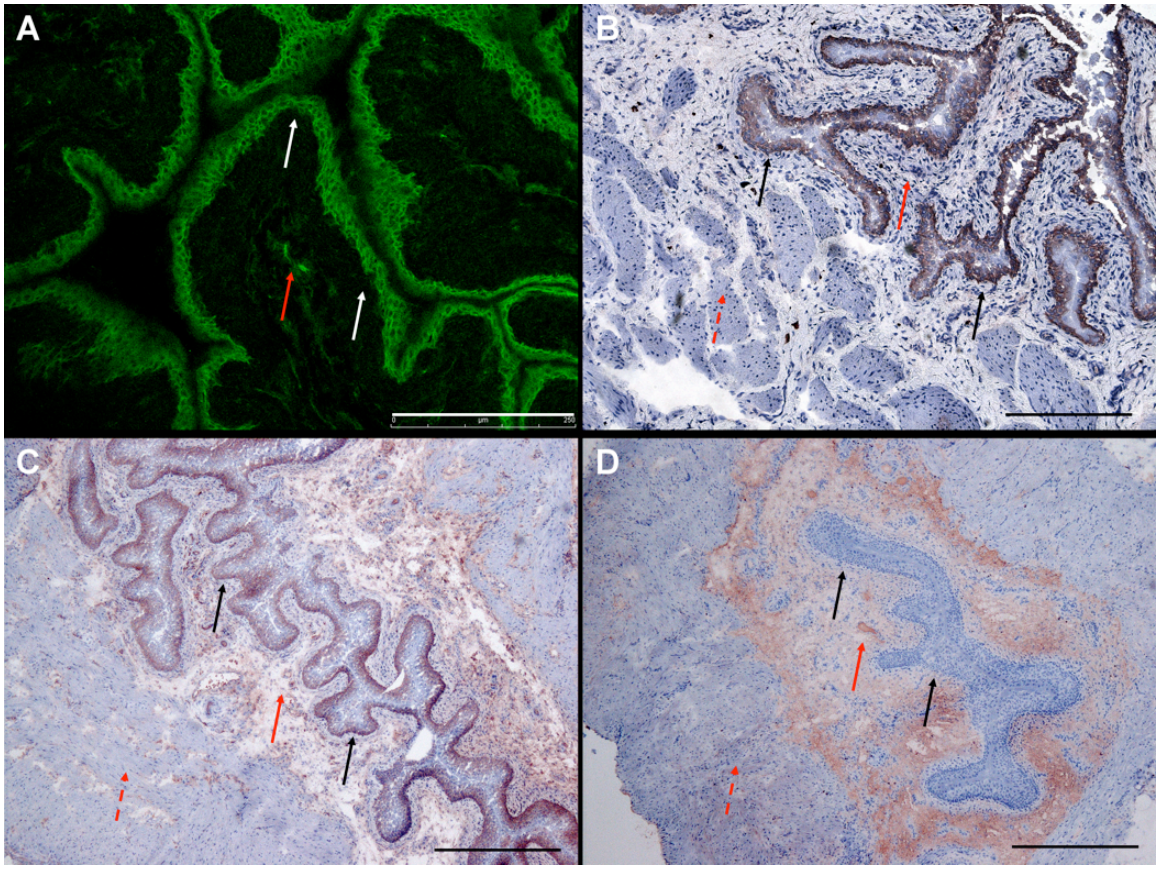

Supplementary Figure 2: Confocal laser scanning microphotographs of rat bladder *(A-B)* and classic immunohistochemistry on full thickness mouse bladder *(C-D)*.

(*A*) TRPV4-immunofluorescence on rat bladder urothelium (white arrows). Unlike in mouse only sparse non-specific non-TRPV4-immunoreactivity is found in the suburothelial layers (red arrow) (*B*) TRPV4-immunoreactivity on rat bladder urothelium (black arrows). Notice little or no immunoreactivity in the suburothelium (full red arrow) and the detrusor (broken red arrow). *(C)* TRPV4-immunoreactivity on urothelium from

full thickness wild type mouse bladder (black arrows). Notice non-specific immunoreactivity in the suburothelium (full red arrow) and the detrusor region (broken red arrow). *(D)* Absence of TRPV4-immunoreactivity on urothelium from full thickness *TRPV4*$^{-/-}$ mouse bladder (black arrows). Notice non-specific immunoreactivity in the suburothelium (full red arrow) and the detrusor region (broken red arrow). Scale bars equal 250µm (A) and 500µm (B-D).

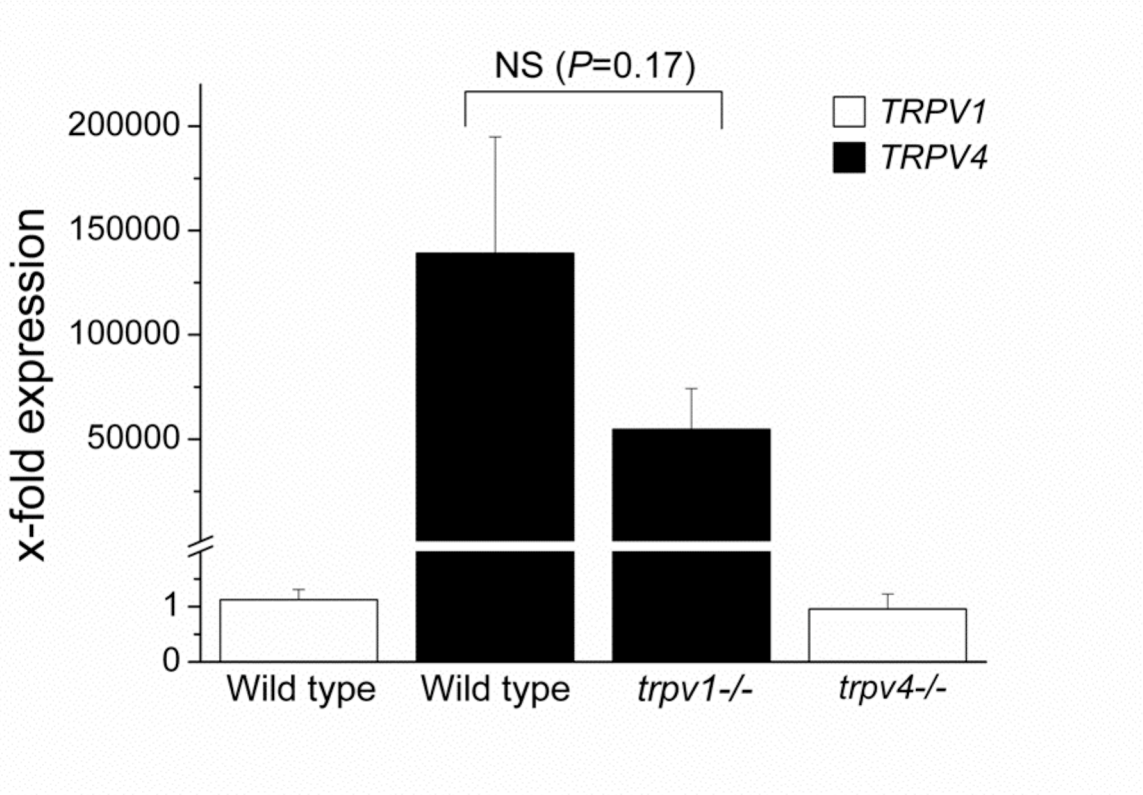

Supplementary Figure 3: Relative quantification of mTRPV1 and mTRPV4 mRNA expression in urothelium of wild type, *TRPV4*$^{-/-}$ and *TRPV1*$^{-/-}$ mice. Data are expressed as ×-fold expression of detected mRNA normalized to TRPV1 mRNA in the *TRPV4*$^{-/-}$ mice, which was used as a calibrator for the comparative ΔΔCt analysis. Data from 4 animals

for each group. All data are means + S.E.M., statistics with unpaired Student's t-test, significance at $P<0.05$.

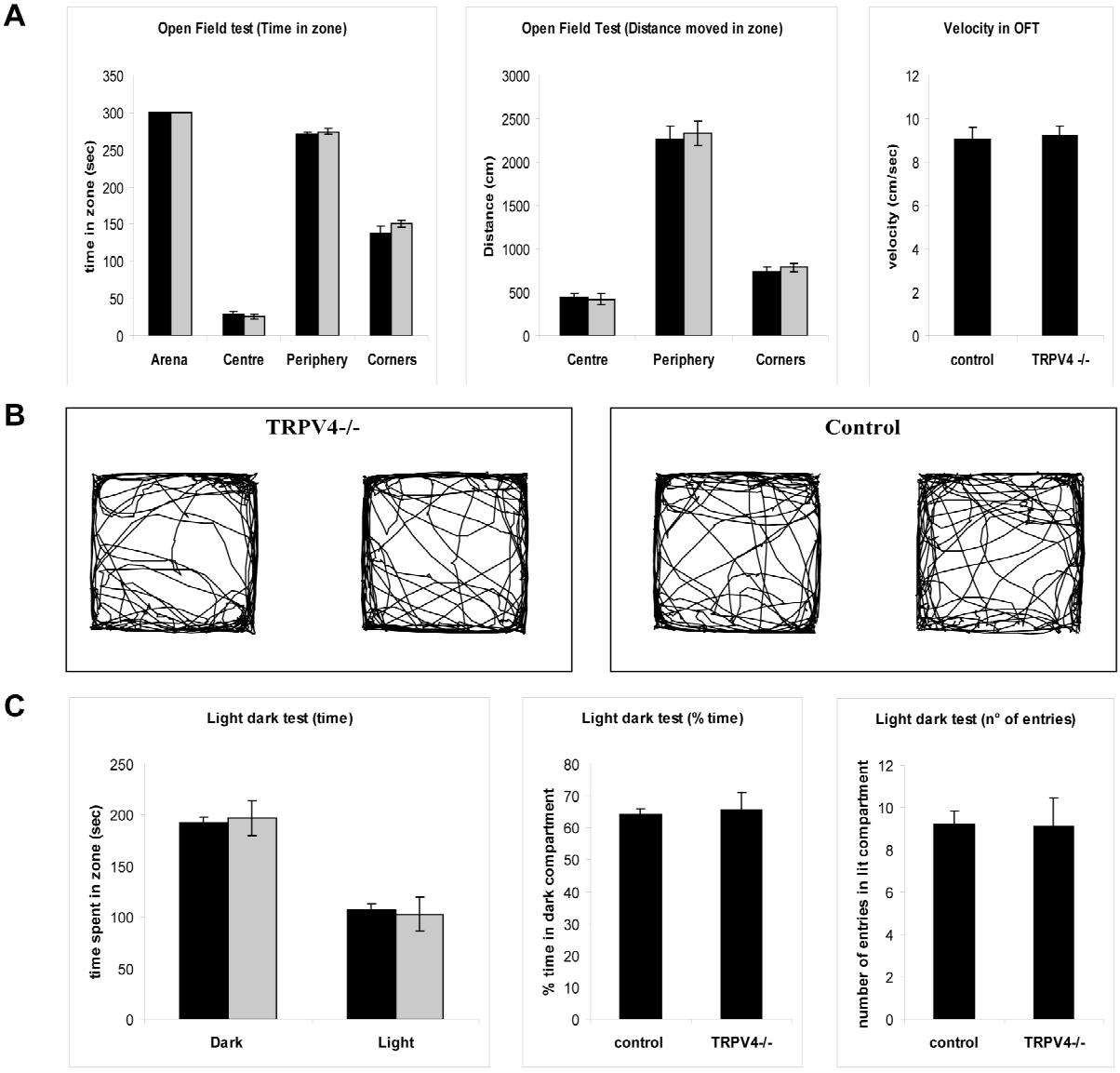

Supplementary Figure 4: Behavioral analysis of *TRPV4*$^{-/-}$ mice in Open-field test *(A-B)* and light/dark test *(C)*. *(A)* Open field activity of *TRPV4*$^{-/-}$ mice and control mice, graphs present (i) time spent in the centre, periphery and corner zones in the corner zones (A, left panel), (ii) Distance moved in the centre, periphery and corner zones (A, middle panel)

and (iii) velocity (A, right panel). *(B)* Representative images of the mouse traveling patterns of 2 mice of each group are presented. *(C)*. Light/dark test of *TRPV4*$^{-/-}$ and control mice graphs present (i) time spent in the lit and dark compartment (C, left panel), (ii) percentage of time spent in the dark compartment (C, middle panel) and (iii) the number of entries in the lit compartment (C, right panel). Data from 10 animals for each group. All data are means + S.E.M., statistics with unpaired Student's t-test, significance at $P<0.05$.